This article has been accepted for publication in IEEE Transactions on Dielectrics and Electrical Insulation. This is the author's version which has not been fully edited and content may change prior to final publication. Citation information: DOI 10.1109/TDEI.2022.3146564

Volume Effect of Dynamic Breakdown Strength in Liquid Nitrogen under Transient Bubble Disturbance for Resistive Superconducting Fault Current Limiters

Naoki Hayakawa, Yuji Mori and **Hiroki Kojima**
Department of Electrical Engineering, Nagoya University
Furo-cho, Chikusa-ku, Nagoya 464-8603, Japan

ABSTRACT

Liquid nitrogen (LN_2) is indispensable as the cooling and electrical insulating materials for high temperature superconducting (HTS) power apparatus. Especially for the resistive superconducting fault current limiters (RSFCL), a transient bubble disturbance in LN_2 is generated due to the quench of HTS materials, which may induce an electrical breakdown in LN_2 even under the rated voltage of RSFCL. We have been investigating not only the intrinsic breakdown characteristics of LN_2 under the steady-state operation but also the dynamic breakdown characteristics of LN_2 under the fault current limiting operation of RSFCL. In this paper, we investigate the heat flux and pressure dependence of the quench-induced dynamic breakdown characteristics of LN_2 by using an actual HTS conductor and a pancake coil model for RSFCL. In addition, the dynamic breakdown strength is discussed and systematized in terms of the volume effect of breakdown strength in LN_2. A flowchart to estimate the intrinsic and dynamic breakdown strength in LN_2 is proposed toward the reliable and rational insulation design of RSFCL.

Index Terms — **liquid nitrogen, breakdown, volume effect, bubble, superconducting fault current limiter**

1 INTRODUCTION

ELECTRICAL insulation systems at cryogenic temperatures have been recognized as one of the common and critical issues for the efficient, reliable and practical development of various superconducting power apparatus, e.g. cables, transformers, fault current limiters (SFCL), generators, motors and magnetic energy storage system (SMES) [1]. Cryogenic liquids such as liquid helium (LHe) and liquid nitrogen (LN_2) are expected as not only cooling media but also electrical insulating media for the superconducting power apparatus. Electrical insulation performance of cryogenic liquids has been investigated toward the reliable, practical and rational development of superconducting power apparatus [2]. However, since the cryogenic liquids have low latent heat, their electrical insulation performance is susceptible to bubbles with low dielectric strength. The bubbles may be generated continuously by heat-in-leak etc. under the steady-state operation or transiently by quench phenomena (transition from superconducting to normal-conducting state) of superconductors under the fault current limiting operation with a larger current than their critical current.

The electrical insulation performance of cryogenic liquids under the steady-state operation can be referred to as "static" or "intrinsic" insulation performance, where microscopic bubbles can be the weak points for electrical insulation. Here, for the conventional power apparatus with dielectric liquids, volume effect of breakdown strength is one of the critical issues to be taken into account for their practical insulation design, where the breakdown strength would decrease with the increase in the highly stressed liquid volume with weak points for electrical insulation. We have already formulated the volume effect of breakdown strength in LHe and LN_2 [3]. Especially, the volume effect in sub-cooled LN_2 under pressurized conditions has been systematized for high temperature superconducting (HTS) power apparatus [4].

On the other hand, the electrical insulation performance of cryogenic liquids under the bubble disturbance may be drastically reduced from the intrinsic one, because the quench-induced bubbles will be transiently generated, but their size and number are much larger than those under the steady-state operation. This is peculiar to superconducting power apparatus and can be referred to as "dynamic" insulation performance. We have also investigated the fundamental dynamic insulation performance of LHe [5] and LN_2 [6]. The dynamic insulation performance of cryogenic liquids is crucial especially for resistive SFCL (RSFCL), which is

Manuscript received on 2 August 2021, in final form 20 December 2021, accepted 3 January 2022. Corresponding author: N. Hayakawa.

© 2022 IEEE. Personal use is permitted, but republication/redistribution requires IEEE permission. See https://www.ieee.org/publications/rights/index.html for more information.

This article has been accepted for publication in IEEE Transactions on Dielectrics and Electrical Insulation. This is the author's version which has not been fully edited and content may change prior to final publication. Citation information: DOI 10.1109/TDEI.2022.3146564

expected to rapidly limit a large fault current in an electric power network by utilizing the quench-induced resistance of superconductors [7, 8]. Without enough consideration on the dynamic insulation performance of cryogenic liquids, RSFCL may be broken at the fault current limiting operation even under the operating voltage. Electrical insulation design of RSFCL under continuously generated bubbles or entire gaseous atmosphere might be possible and safe, but too conservative and pessimistic. Therefore, the dynamic insulation performance of cryogenic liquids is essential and worthy to be investigated for the reliable, practical and rational insulation design of RSFCL.

Researches on the dynamic breakdown characteristics of LN_2 have been recently activated, e.g. under sphere-plane electrode at long gap length [9], turn-to-turn electrode for a pancake coil model for RSFCL [10], insulating paper under boiling [11], and so on. Dynamic breakdown characteristics in such researches have been obtained by using conventional heaters to generate bubbles in LN_2. However, for the reliable and practical insulation design of RSFCL, it is preferable to investigate the dynamic breakdown characteristics of LN_2 by using actual quench of HTS conductors and coils for RSFCL.

From the above background, in this paper, using an actual HTS conductor and a pancake coil model, we obtained the quench-induced dynamic breakdown characteristics of LN_2 for different heat flux from the HTS conductors at the different LN_2 pressures. In addition, we discussed and systematized the dynamic breakdown strength in terms of the volume effect of breakdown strength in LN_2. Finally, we proposed a flowchart to evaluate the intrinsic and dynamic breakdown strength in consideration of their volume effect for the reliable, practical and rational insulation design of RSFCL.

2 EXPERIMENTAL SETUP AND METHODS

2.1 HTS PANCAKE COIL MODEL

Figure 1 shows the HTS pancake coil model. The HTS pancake coil model is composed of bifilarly wound 2 tapes, i.e. HTS and nichrome tapes, as a fundamental coil configuration

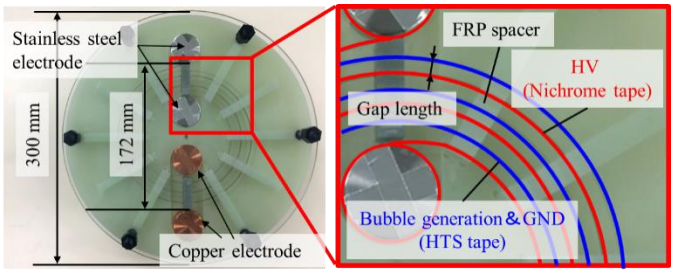

Figure 1. HTS pancake coil model.

Table 1. Specifications of HTS tapes.

	Material	Thickness [μm]
Stabilizer	Ag	2
HTS layer	GdBCO	3-4
Buffer layer	CeO_2/Y_2O_3	0.3
Substrate	Ni/Cu/SUS	2/48/100
Width [mm]	4	
Total thickness [mm]	0.18	
Critical current I_c [A]	113-116	
n value	23.8-28.8	

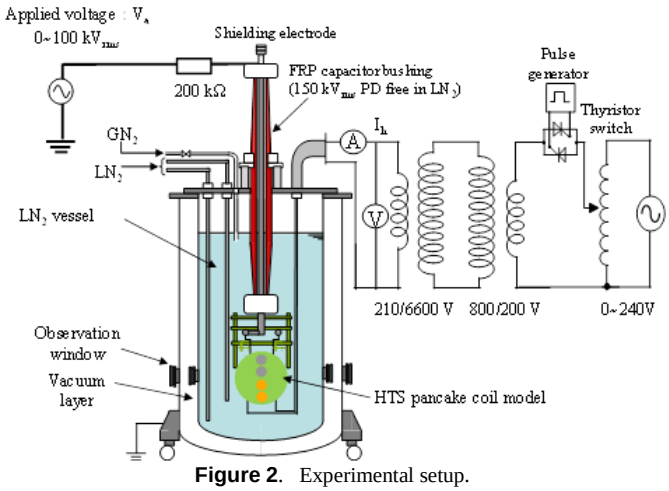

Figure 2. Experimental setup.

of RSFCL. Table 1 shows the specifications of the HTS tapes. When a current enough larger than the critical current is applied to the HTS tapes in LN_2, the HTS tapes will be quenched and bubbles are transiently generated in LN_2 until the current is interrupted. The nichrome tapes have the same width of 4 mm as that of HTS tapes. Both tapes are bifilarly wound by 3 turns, respectively, with the gap length of 6 mm between the adjacent tapes and supported by FRP (fiber reinforced plastic) spacers. The HTS and nichrome tapes are connected to the copper and stainless steel bulk electrodes, respectively. The HTS pancake coil model is sandwiched between FRP and PET (polyethylene terephthalate) plates to observe the bubble disturbance in LN_2. The model was arranged vertically in the cryostat, because the intrinsic and dynamic breakdown strengths of vertical arrangement were higher than those of horizontal arrangement, which will be better for RSFCL [6].

2.2 EXPERIMENTAL SETUP

Figure 2 shows the experimental setup. The cryostat has inner and outer vessels, and the HTS pancake coil model is installed in the inner vessel, which can be pressurized by N_2 gas up to the absolute pressure P = 0.5 MPa. The temperature T in the inner cryostat is fixed at T = 77 K by atmospheric LN_2 in the outer vessel. The cryostat also has a FRP capacitor bushing, which is partial discharge free at 150 kV_{rms} in LN_2.

A high voltage (ac 60 Hz) is applied to the nichrome tapes of the HTS pancake coil model, whereas the HTS tapes are grounded. A large current (ac 60 Hz) controlled by a thyristor switch and a transformer is applied to the HTS tapes to be quenched. The heat flux Q [W/cm^2] generated from the HTS tapes in the quench condition is defined as the first peak of the product of current and voltage across the HTS tapes. For the calculation of Q, we used the area of entire HTS tape surface under the assumption that the quench was uniformly generated in the coil model, because (1) the applied current to the HTS tapes is enough larger than the critical current of 113-116 A in Table 1, (2) the bubble disturbance was generated from the most area of HTS tapes and (3) the locations of dynamic breakdown were distributed at different points of HTS tapes.

In this paper, we carried out the experiments for P=0.10, 0.12, 0.15 MPa and Q=0–80 W/cm^2 at T=77 K. Figure 3 shows an example of voltage, current and heat flux waveforms at the quench of HTS tapes at Q=33.7 W/cm^2.

© 2022 IEEE. Personal use is permitted, but republication/redistribution requires IEEE permission. See https://www.ieee.org/publications/rights/index.html for more information.

This article has been accepted for publication in IEEE Transactions on Dielectrics and Electrical Insulation. This is the author's version which has not been fully edited and content may change prior to final publication. Citation information: DOI 10.1109/TDEI.2022.3146564

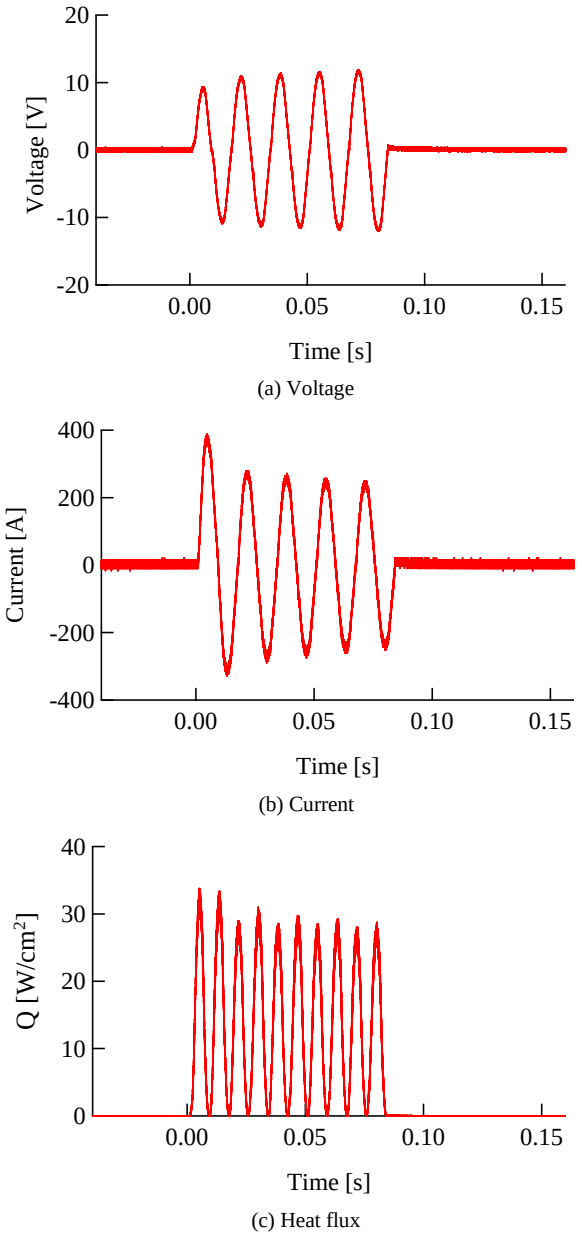

Figure 3. Voltage, current and heat flux waveforms at the quench of HTS tapes (Q=33.7 W/cm^2).

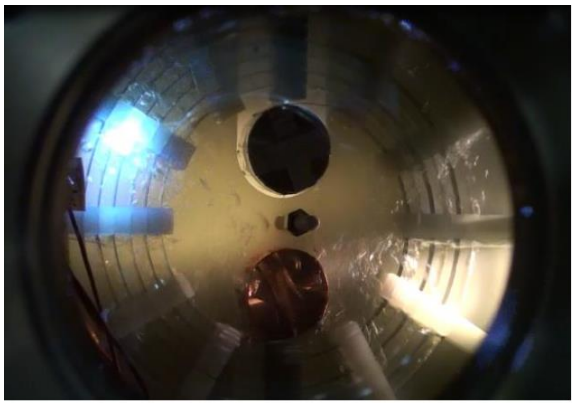

Figure 4. Dynamic breakdown of HTS pancake coil (V_a=15.6 kV, Q=48.7 W/cm^2).

2.3 EXPERIMENTAL METHOD

Firstly, we gradually increased the applied voltage to the nichrome tapes at 1 kV$_{rms}$/s until a breakdown occurs without applying current to the HTS tapes. We repeatedly measured the breakdown voltage 10 times under the same condition. We calculated the intrinsic breakdown voltage $V_{intrinsic}$ with the probability of 50 % by the Weibull analysis, and converted $V_{intrinsic}$ to the intrinsic breakdown strength $E_{intrinsic}$ at the tape edges with the probability of 50 % by electric field analysis with finite element method (FEM).

Next, we exposed the HTS pancake coil model to a high electric field strength at the applied voltage V_a below $V_{intrinsic}$. Then, we applied a current larger than the critical current to the HTS tapes for 5 cycles in order to induce quench and transient bubble disturbance in LN_2. We repeatedly induced the quench 10 times at the fixed V_a and Q, then obtained the probability of dynamic breakdown. Figure 4 shows an example of dynamic breakdown at V_a=15.6 kV, Q=48.7 W/cm^2. We repeated this operation for different V_a to get the dynamic breakdown probability at each V_a. From the relationship between the dynamic breakdown probability and V_a, we calculated the dynamic breakdown voltage $V_{dynamic}$ and strength $E_{dynamic}$ at the tape edges with the probability of 50 %.

The voltage, current and heat flux waveforms of HTS tapes in Figure 3 and the bubble behavior in the dynamic breakdown test in Figure 4 were reproducible under the repeated breakdowns, because the intrinsic or dynamic breakdown current is enough suppressed by the resistance 200 kΩ in the high voltage circuit in Figure 2. These results mean that the damage to the HTS tapes was not caused by the breakdowns and the measured values can be used to obtain the statistical results.

3 EXPERIMENTAL RESULTS AND DISCUSSIONS

3.1 HEAT FLUX AND PRESSURE DEPENDENCE OF DYNAMIC BREAKDOWN STRENGTH

Figure 5 shows the experimental results for the heat flux and pressure dependence of $E_{intrinsic}$ and $E_{dynamic}$ in the HTS pancake coil model. $E_{dynamic}$ decreases remarkably from $E_{intrinsic}$ with the

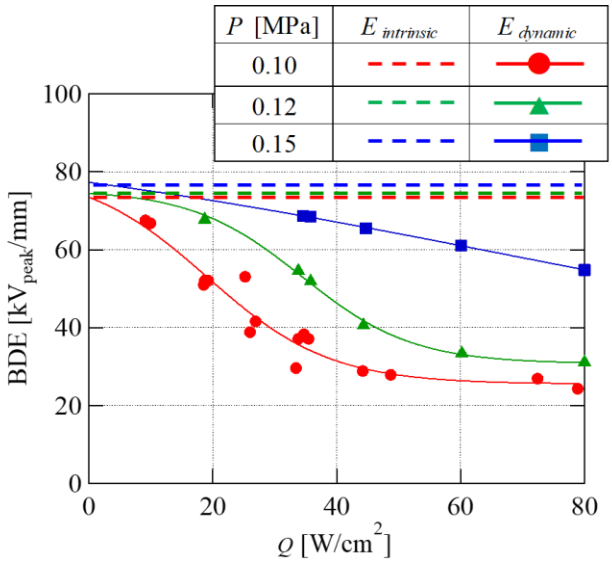

Figure 5. Pressure and heat flux dependence of breakdown strength.

© 2022 IEEE. Personal use is permitted, but republication/redistribution requires IEEE permission. See https://www.ieee.org/publications/rights/index.html for more information.

This article has been accepted for publication in IEEE Transactions on Dielectrics and Electrical Insulation. This is the author's version which has not been fully edited and content may change prior to final publication. Citation information: DOI 10.1109/TDEI.2022.3146564

increase in heat flux, since the size and number of bubbles increase with the increase in heat flux. In addition, the higher pressure increases $E_{dynamic}$, since the size and number of bubbles decrease with the increase in pressure.

$E_{dynamic}$ is almost constant at Q > 40 W/cm^2 in 0.10 MPa and at Q > 60 W/cm^2 in 0.12 MPa. $E_{dynamic}$ would reach the lower limit in LN_2 filled with bubbles between the adjacent tapes with the increase in heat flux. The pressure dependence of the lower limit would be attributed to the bubble density in LN_2.

3.2 VOLUME EFFECT OF DYNAMIC BREAKDOWN STRENGTH IN LN_2

The solid and dotted lines in Figure 6 show the volume effect of $E_{intrinsic}$ in LN_2 [4]. The horizontal axis, α%SLV, is the stressed liquid volume (SLV) with the high electric field strength exceeding a certain ratio (α%) with respect to the maximum electric field strength. α = 81% has been obtained at 0.10 MPa and 77 K in the boiling state of atmospheric LN_2. $E_{intrinsic}$ decreases with the increase in α%SLV, since the intrinsic breakdown depends on the size and number of microscopic bubbles as the weak points in electrical insulation existing in the high electric field region, i.e. α%SLV, in LN_2. The value of α or α%SLV is a function of pressure and temperature of LN_2 for $E_{intrinsic}$ [4]. Figure 7 shows an example

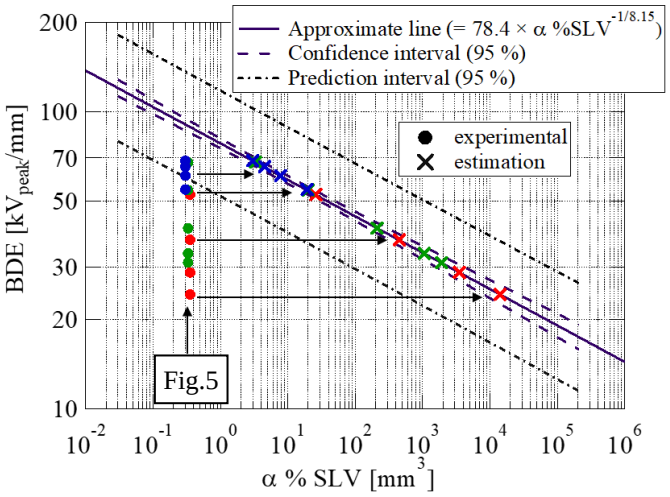

Figure 6. Breakdown strength as a function of α%SLV.

Test sample	Pancake coil
T [K]	77
P [MPa]	0.1
α [%]	81
g [mm]	2
V_a [kV$_{peak}$]	23.2
ζ	0.187

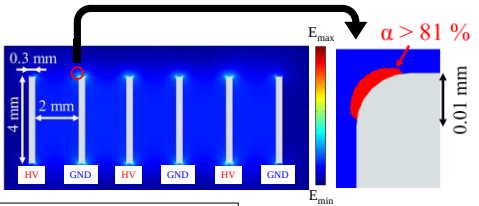

1) Calculate E_{max} by electric field analysis with minimum mesh size of 0.002 mm (2D object). → E_{max} = 76.0 kV$_{peak}$/mm

2) Pick up the meshes with the electric field strength E_a at each mesh greater than 0.81 × 76.0 = 61.6 kV$_{peak}$/mm.

3) Integrate the area (1.5E-4 mm^2) of the meshes picked up at 2) and multiply the coil length (1808 mm, measured).

→ α%SLV = 0.27 mm^3

Figure 7. Calculation process of α%SLV (Gap length: 2 mm) [6]

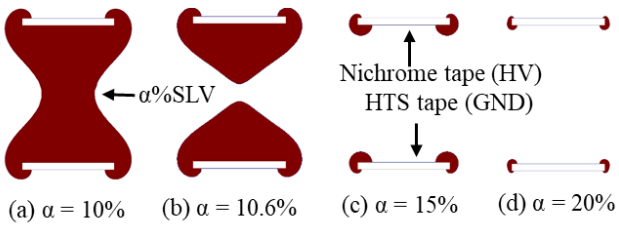

Figure 8. High electric field region (α%SLV) for different values of α.

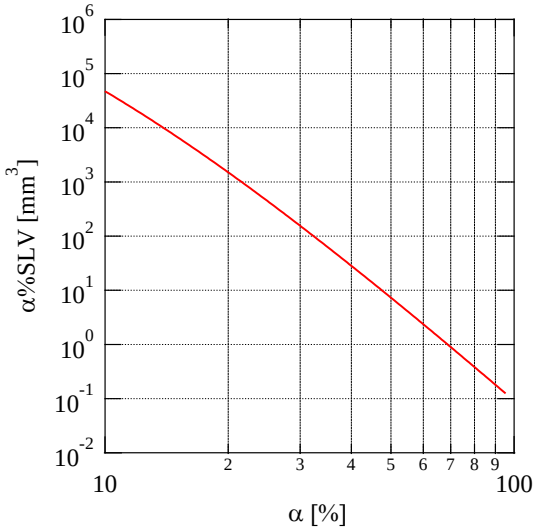

Figure 9. α%SLV as function of α for HTS pancake coil model.

of calculation process of α%SLV for a pancake coil model with the gap length of 2 mm [6].

On the other hand, the dynamic breakdown is induced by macroscopic bubbles due to the quench of HTS tapes. Then, the decrease in $E_{dynamic}$ with the increase in heat flux in Figure 5 can be considered to be equivalent to the increase in α%SLV. α%SLV of the HTS pancake coil model in Figure 1 corresponds to the limited region around the tape edge [6]. Figure 8 shows the region of α%SLV for the HTS pancake coil model between the adjacent tapes for different values of α. In addition, Figure 9 shows α%SLV as a function of α. These figures were

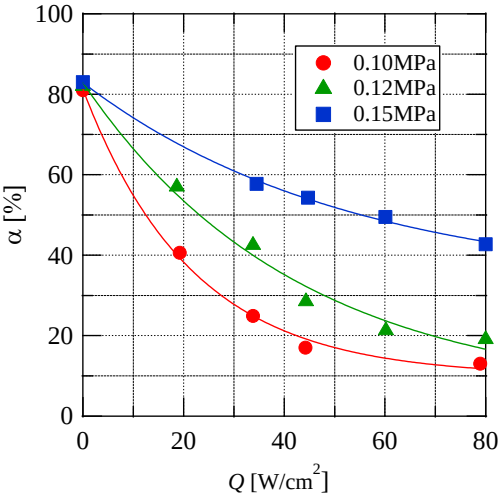

Figure 10. Pressure and heat flux dependence of α for HTS pancake coil model.

© 2022 IEEE. Personal use is permitted, but republication/redistribution requires IEEE permission. See https://www.ieee.org/publications/rights/index.html for more information.

This article has been accepted for publication in IEEE Transactions on Dielectrics and Electrical Insulation. This is the author's version which has not been fully edited and content may change prior to final publication. Citation information: DOI 10.1109/TDEI.2022.3146564

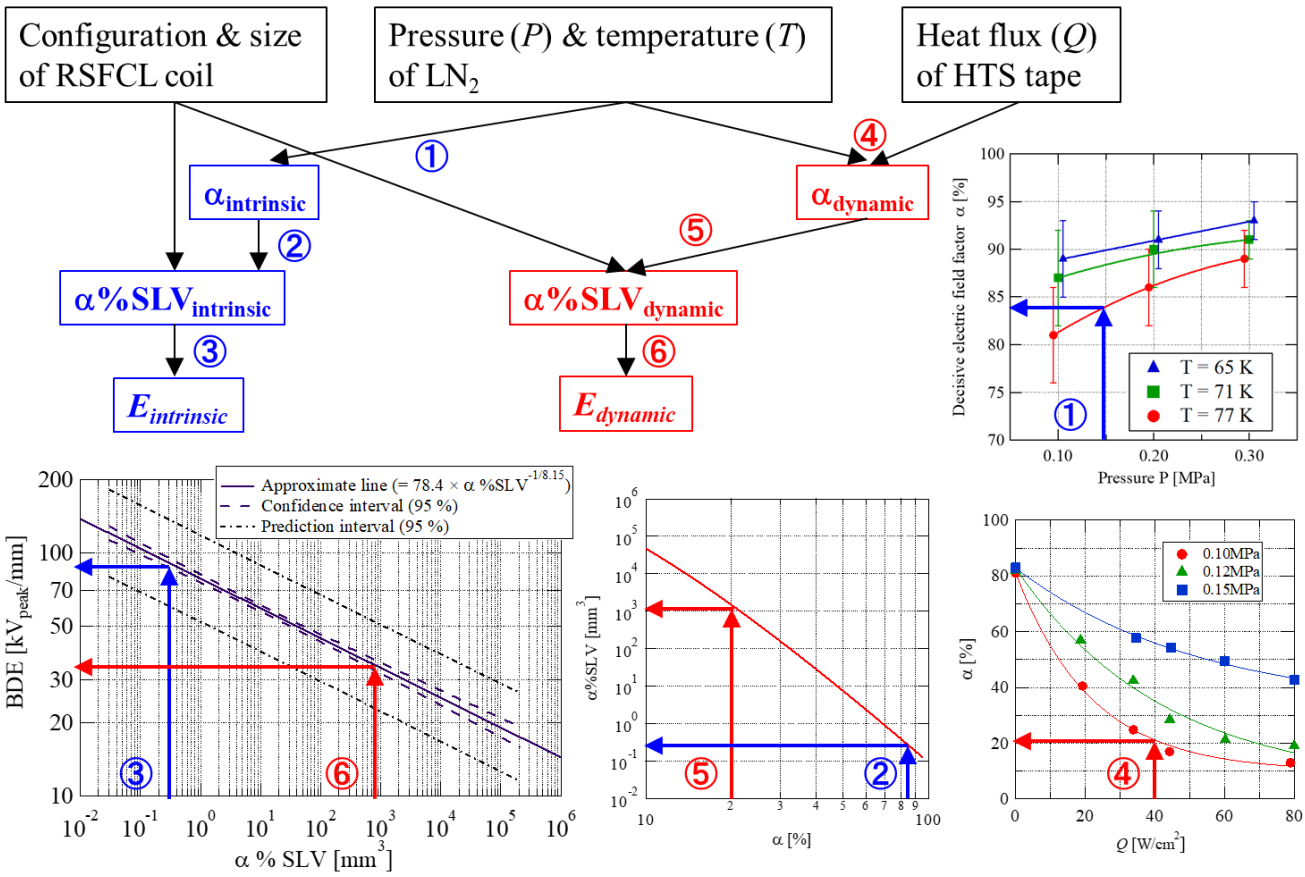

Figure 11. Flowchart to estimate $E_{intrinsic}$ and $E_{dynamic}$ for RSFCL.

calculated by electric field analysis with finite element method (FEM) for the HTS pancake coil model in Figure 1. From these figures, α%SLV sharply increases with the decrease in α, and α%SLV at α = 10% is almost whole region between the adjacent tapes, leading to dynamic breakdown.

From the above concept and procedure, Figure 10 is obtained as the heat flux and pressure dependence of α. The value of α was derived from Figures 6 and 9, and the value of Q came from Figure 5. In Figure 10, α decreases to about 10% at Q = 80 W/cm^2 and P = 0.10 MPa, but increases to about 40% at P = 0.15 MPa. As a result, $E_{dynamic}$ can be obtained as a function of pressure P, temperature T of LN_2 and the heat flux Q at the quench of HTS tapes.

3.3 FLOWCHART TO ESTIMATE INTRINSIC AND DYNAMIC BREAKDOWN STRENGTH

By using the graphs obtained in this paper and the previous paper [4], a flowchart to estimate $E_{intrinsic}$ and $E_{dynamic}$ for RSFCL is summarized in Figure 11:

(1) $\alpha_{intrinsic}$ can be obtained from the pressure P and temperature T of LN_2 using the α-P graph in [4], e.g. $\alpha_{intrinsic}$=84 % when RSFCL will be operated at P=0.15 MPa and T=77 K.

(2) $\alpha\%SLV_{intrinsic}$ can be calculated by the electric field analysis with the configuration and size of RSFCL coil and $\alpha_{intrinsic}$ obtained in (1), e.g. $\alpha\%SLV_{intrinsic}=2.8\times10^{-1}$ mm^3 at $\alpha_{intrinsic}$=84 % in Figure 9 for the HTS pancake coil model in this paper.

(3) $E_{intrinsic}$ can be estimated from $\alpha\%SLV_{intrinsic}$ obtained in (2), e.g. $E_{intrinsic}$=92 kV$_{peak}$/mm at $\alpha\%SLV_{intrinsic}=2.8\times10^{-1}$ mm^3 in Figure 6.

(4) $\alpha_{dynamic}$ can be obtained in Figure 10 for the pressure P, temperature T of LN_2 and the estimated heat flux Q at the quench of HTS tapes, e.g. $\alpha_{dynamic}$=21 % when Q=40 W/cm^2 is estimated.

(5) $\alpha\%SLV_{dynamic}$ can be calculated from $\alpha_{dynamic}$ obtained in (4) for the same RSFCL coil, e.g. $\alpha_{dynamic}=1.2\times10^{3}$ mm^3 at $\alpha_{dynamic}$=21 % in Figure 9.

(6) $E_{dynamic}$ can be estimated from $\alpha\%SLV_{dynamic}$ obtained in (5), e.g. $E_{dynamic}$=33 kV$_{peak}$/mm at $\alpha\%SLV_{dynamic}=1.2\times10^{3}$ mm^3 in Figure 6.

From the above procedure, $E_{dynamic}$ can be estimated to be reduced to 36 % (=33/92) of $E_{intrinsic}$ at P=0.15 MPa, T=77 K and Q=40 W/cm^2 for the HTS pancake coil model in Figure 1. If the intrinsic and dynamic breakdown characteristics will be complemented for different conditions of LN_2, HTS tapes and coils in the similar way as this paper, the reliable and rational insulation design of practical RSFCL will be possible.

4 CONCLUSIONS

We investigated the quench-induced dynamic breakdown characteristics of LN_2 under the transient bubble disturbance for resistive superconducting fault current limiters (RSFCL) and discussed in terms of volume effect of breakdown strength. The main results are summarized as follows:

© 2022 IEEE. Personal use is permitted, but republication/redistribution requires IEEE permission. See https://www.ieee.org/publications/rights/index.html for more information.

This article has been accepted for publication in IEEE Transactions on Dielectrics and Electrical Insulation. This is the author's version which has not been fully edited and content may change prior to final publication. Citation information: DOI 10.1109/TDEI.2022.3146564

(1) The dynamic breakdown strength $E_{dynamic}$ in LN_2 decreases remarkably from the intrinsic breakdown strength $E_{intrinsic}$ with the increase in the heat flux, since the size and number of bubbles increase with the increase in heat flux. In addition, the higher pressure increases $E_{dynamic}$, since the size and number of bubbles decrease with the increase in pressure.
(2) $E_{dynamic}$ can be evaluated in terms of volume effect of breakdown strength in LN_2 by equivalently increasing the stressed liquid volume (α%SLV) for $E_{intrinsic}$ to those for $E_{dynamic}$.
(3) $E_{dynamic}$ can be obtained as a function of pressure P, temperature T of LN_2 and the heat flux Q at the quench of HTS tapes.
(4) A flowchart to estimate $E_{intrinsic}$ and $E_{dynamic}$ in LN_2 is proposed in consideration of their volume effect.

These results will contribute to the reliable and rational insulation design of RSFCL based on both the intrinsic and dynamic breakdown characteristics of LN_2.

ACKNOWLEDGMENT

This work was supported by JSPS KAKENHI Grant Number JP17H03215.

REFERENCES

[1] M. Noe *et al*, "Common Characteristics and Emerging Test Techniques for High Temperature Superconducting Power Equipment," *CIGRE Working Group D1.38 Technical Brochure*, no. 644, 2015.
[2] I. Sauers *et al*, "Effect of Bubbles on Liquid Nitrogen Breakdown in Plane-Plane Electrode Geometry from 100-250kPa," *IEEE Trans. Appl. Supercond.*, vol. 21, no. 3, pp. 1892-1895, Jun. 2011.
[3] H. Okubo *et al*, "High Voltage Insulation Performance of Cryogenic Liquids for Superconducting Power Apparatus," *IEEE Trans. Power Delivery*, vol. 11, no. 3, pp. 1400-1406, Jul. 1996.
[4] N. Hayakawa *et al*, "Size Effect on Breakdown Strength in Sub-cooled Liquid Nitrogen for Superconducting Power Apparatus," *IEEE Trans. Dielectr. Electr. Insul*., vol. 22, no. 5, pp. 2565–2571, Oct. 2015.
[5] S. Chigusa, N. Hayakawa, and H. Okubo, "Static and Dynamic Breakdown Characteristics of Liquid Helium for Insulation Design of Superconducting Power Equipment," *IEEE Trans. Dielectr. Electr. Insul*., vol. 7, no. 2, pp. 290-295, Apr. 2000.
[6] N. Hayakawa *et al*, "Dynamic Breakdown Characteristics of Pancake Coil Model for Resistive Superconducting Fault Current Limiters," *IEEE Trans. Appl. Supercond*., vol. 29, no. 5, 5603106, Aug. 2019.
[7] M. Moyzykh *et al*, "Superconducting fault current limiter for Moscow 220 kV city grid," *European Conf. Appl. Supercond. (EUCAS), 2017*, 1LO1-02.
[8] P. Tixador *et al*, "Status of the European union project FASTGRID," *IEEE Trans. Appl. Supercond.*, vol. 29, no. 5, 5603305, Aug. 2019.
[9] S. Fink *et al*, "AC breakdown voltage of liquid nitrogen depending on gas bubbles and pressure," *Int. Conf. High Voltage Eng. and Appl. (ICHVE)*, 2014, 7035445.
[10] R. Chassagnoux *et al*, "Study of turn-to-turn electrical breakdown for superconducting fault current limiter applications," *IEEE Trans. Appl. Supercond.*, vol. 29, no. 5, 7701705, Aug. 2019.
[11] D. Gromoll, R. Schumacher, and C. Humpert, "Dielectric strength of insulating material in LN_2 with thermally induced bubbles," *J. Physics: Conf. Series*, vol. 1559, 012087, 2020.

Naoki Hayakawa (M'90) was born in Japan in 1962. He received his Ph.D degree in 1991 in electrical engineering from Nagoya University. He has been at Nagoya University since 1990, where he is presently a Professor in the Department of Electrical Engineering. From 2001 to 2002, he was a guest scientist at the Forschungszentrum Karlsruhe, Germany. Prof. Hayakawa is a member of IEE of Japan and CIGRE, and the Convenor of CIGRE WG D1.64 on "Electrical Insulation Systems at Cryogenic Temperatures".

Yuji Mori was born in Japan in 1996. He received his MS degree in 2021 in electrical engineering from Nagoya University. He engaged in the researches on dynamic breakdown characteristics of liquid nitrogen and transient stability of power system with superconducting fault current limiters. Mr. Mori is a member of IEE of Japan.

Hiroki Kojima (M'11) was born in Japan in 1975. He received his Ph.D degree in 2004 in energy engineering and science from Nagoya University. He was a Research Fellow with the Japan Society for the Promotion of Science from 2000 to 2003. Since 2004, he has been at Nagoya University and presently he is an Associate Professor of Nagoya University in the Department of Electrical Engineering. Dr. Kojima is a member of IEE of Japan.

© 2022 IEEE. Personal use is permitted, but republication/redistribution requires IEEE permission. See https://www.ieee.org/publications/rights/index.html for more information.